Distance-as-time in physical aging

Ian M. Douglass and Jeppe C. Dyre
Glass and Time, IMFUFA, Department of Science and Environment, Roskilde University, P. O. Box 260, DK-4000 Roskilde, Denmark
(Dated: May 17, 2022)

Although it has been known for half a century that the physical aging of glasses is described by a linear thermal-history convolution integral over the so-called material time, the microscopic interpretation of the material time remains a mystery. We propose that the material time increase over a given time interval reflects the distance traveled by the system's particles. Different possible distance measures are discussed, starting from the standard mean-square displacement. The viewpoint adopted implies a "geometric reversibility" and a "unique-triangle property" characterizing the system's path in configuration space during aging, both of which properties are inherited from equilibrium and confirmed by computer simulations of an aging binary Lennard-Jones system. The simulations show that the slow particles control the material time. This motivates a dynamic-rigidity-percolation picture of physical aging; specifically the material time is proposed to be a function of the slowest quartile particles' inherent square displacement. This collapses well numerical data for the potential energy during aging in the sense that the normalized relaxation function following any temperature jump is almost the same function of this material time. The standard Tool-Narayanaswamy equation for physical aging is arrived at by assuming that when time is replaced by distance, an aging system is described by the same expression as that of linear-response theory.

I. INTRODUCTION

What is the time? This is, in brief, the guiding question of the present paper. When material properties change over the coarse of time as a consequence of molecular reorganization, the term "physical aging" is used [1–23]. An example is that of a glass kept slightly below the glass-transition temperature. As pointed out by Simon long ago [1], such a system approaches very slowly the equilibrium metastable liquid state. Physical aging is important in both production and subsequent use of three large classes of materials: covalently bonded inorganic glasses [4–6, 9, 24], polymers [3, 7, 10, 17, 25–28], and metallic glasses [20, 29–35]. Besides these quite different materials, the same qualitative aging phenomena have been reported for, e.g., spin glasses [36, 37], relaxor ferroelectrics [38], soft glassy materials like colloids and gels [39–41], and active matter [42, 43].

The properties of a glass depends generally on its thermal history after falling out of equilibrium at the glass transition, and the rate of physical aging also depends on this history [9, 17, 44–47]. From a theoretical perspective, physical aging may be regarded as an instance of response theory that considers how a given physical quantity, the "output", responds to an externally controlled "input" which in aging is usually the temperature history, but also can be, e.g., the pressure history of a combination thereof. Close to the glass transition temperature, even small temperature changes result in several orders of magnitude variation of the average relaxation time. This is why physical aging is generally strongly *nonlinear* in the sense that property changes cannot be calculated from a standard linear convolution integral over the temperature variation (unless this is significantly smaller than one percent) [9, 17, 21].

Examples of properties monitored in experimental studies of physical aging are: density, enthalpy, viscosity, index of diffraction, dc conductivity, frequency-dependent or nonlinear dielectric properties, elastic moduli, and structure probed by X-rays [3, 4, 7, 29, 48–58]. The simplest temperature protocol for studying physical aging is that of a temperature jump. An ideal jump starts from a state of thermal equilibrium after which the system is monitored until it reaches equilibrium at the so-called annealing temperature [3, 4, 9]. The response to both up and down jumps is generally nonexponential in time [9]. Comparing jumps to the same temperature, a jump from above approaches equilibrium considerably faster and more stretched than one from below [3, 9, 28, 59, 60]. The former is referred to as self-retarded, the latter as self-accelerated [28]. This "asymmetry of approach" [3, 17] has long been understood as an effect of the so-called fictive temperature reflecting the glass structure and controlling the aging rate, a quantity that equals the temperature for systems in thermal equilibrium [9, 17, 59]. The fictive temperature decreases following a down jump in temperature, which results in initially fast aging that gradually slows down. For an up jump the opposite happens [3, 9, 10, 17]. Only for very small temperature jumps does one enter into a virtually linear regime for which up and down jumps are mirror images of one another; here standard linear-response theory applies as recently demonstrated experimentally [23, 61].

In 1971 the Ford Motor Company engineer Narayanaswamy rationalized the asymmetry of approach by replacing the actual time t with a "material" time ξ [4]. As a sample ages, the rate at which the material time increases changes itself. The beauty of the Narayanaswamy idea is that the function $\xi(t)$ embodies all nonlinear effects of the sample thermal history [9]. Thus a linear description is arrived at if ξ instead of t is the time variable, and almost miraculously the asymmetry between up and down jumps disappears [4, 8, 9]. The formalization of Narayanaswamy's seminal discovery is nowadays referred to as the Tool-Narayanaswamy (TN) formalism [4, 9, 59]. It not only accounts for the asymmetry of approach [3, 17], but also for all other characteristics of physical aging, e.g., the noted Ritland-Kovacs crossover experiment [3, 9, 62].

The TN formalism was devised for optimizing the cooling rate of windshields during production [4]. A few years later, a mathematically equivalent approach was introduced for polymers [8], which have the same aging characteristics as oxide and other covalently bonded glasses. Because of its good description of physical aging, the TN formalism has been used for decades in industry. In academia, on the other hand, there has been limited interest in developing and further refining this approach to physical aging. This is the case even though many aspects of physical aging are still not well understood, a major challenge being simply to explain why the TN formalism works so well.

Aging papers often focus on identifying how the aging rate $d\xi/dt$ varies with macroscopic quantities like density, enthalpy, configurational entropy, high-frequency plateau shear modulus, etc [4, 9, 17, 63, 64]. The present paper does not address this important problem, but focuses on the material-time concept itself. To be specific, the TN-formalism raises a number of fundamental questions that after 50 years remain unanswered, for instance: Why can the highly nonlinear physical-aging phenomenon be described by linear mathematics? How can the material time be related to microscopic quantities? Why is aging of different quantities usually controlled by the same material time? Why does the TN formalism work best for small temperature variations?

The main idea of the present paper is that the material time reflects the distance traveled of the system in configuration space. As discussed in Sec. V A, similar "distance-as-time" ideas have been proposed throughout the years in various contexts [65–69]. To the best of our knowledge, however, the distance-as-time approach has not been related to the TN formalism. The material-time concept is known to work best for relatively small temperature variations,

i.e., for systems that are only weakly out of equilibrium [9, 17, 61], and this is the present focus. Thus we are not attempting to construct a completely general theory of physical aging. The regime of relatively mild thermodynamic perturbation is nevertheless strongly nonlinear in the mathematical sense, which is the relevant regime for the modeling of many experiments, e.g., that of continuous cooling through the glass transition.

We find below that the standard mean-square displacement distance does not work well as the quantity controlling the material time. The inherent distance traveled by the slowest quarter particles is a significantly better candidate for defining the material time. Our investigation demonstrates a nontrivial "geometric reversibility" of physical aging, which is closely related to the triangular relation between aging time-autocorrelation functions of spin-glass models derived theoretically long ago by Cugliandolo, Kurchan, and coworkers [65, 66, 70]. Finally, we rewrite standard linear-response theory in terms of the distance measure and show that the TN formalism follows from the assumption that the same equation applies for aging systems.

II. DISTANCE-AS-TIME IN THERMAL EQUILIBRIUM

This section motivates the use of displacement to define the material time of an aging system by discussing equilibrium results, which are trivial in the sense that they are straightforward to prove rigorously.

Consider a system of N particles in volume V in thermal equilibrium. The particle positions define the collective $3N$-dimensional coordinate vector $\mathbf{R} \equiv (\mathbf{r}_1, ..., \mathbf{r}_N)$. The system traces out a trajectory in configuration space, $\mathbf{R}(t)$. For any two times t_1 and t_2 we define the distance d_{12} between the configurations $\mathbf{R}_1 = \mathbf{R}(t_1)$ and $\mathbf{R}_2 = \mathbf{R}(t_2)$ by the mean-square displacement (MSD)

$$d_{12} \;=\; \frac{(\mathbf{R}_2 - \mathbf{R}_1)^2}{N}\,. \tag{1}$$

This distance measure has the property that it for widely separated times is proportional to the time difference, i.e.,

$$d_{12} \;\propto\; |t_2 - t_1| \;\text{ for } |t_2 - t_1| \to \infty\,. \tag{2}$$

In the thermodynamic limit, relative fluctuations of $(\mathbf{R}_2 - \mathbf{R}_1)^2$ deriving from finite size effects and different thermal velocities go to zero, implying that d_{12} is a unique function of $|t_2 - t_1|$. Conversely, $|t_2 - t_1|$ is a unique function of d_{12}. Henceforth, we have the thermodynamic limit in mind and ignore distance fluctuations. All four distance measures discussed below obey Eq. (2), which is crucial for deriving the TN equation (Sec. V B).

For any three times $t_1 < t_2 < t_3$ the coordinate vectors $\mathbf{R}_1$, $\mathbf{R}_2$, and $\mathbf{R}_3$ define a triangle in configuration space. Because the MSD increases monotonically with time, each side length determines the corresponding time difference. This implies that the triangle has the "unique-triangle property" [71]: knowledge of any two side lengths determines the third. For instance, if d_{12} and d_{23} are known, $t_2 - t_1$ and $t_3 - t_2$ are known, which implies a knowledge of $t_3 - t_1 = t_3 - t_2 + t_2 - t_1$ and thereby of d_{13}. The unique-triangle property may be summarized by writing (in which F is a function that may vary with system and thermodynamic state point)

$$d_{13} \;=\; F(d_{12}, d_{23}) \;=\; F(d_{23}, d_{12})\,. \tag{3}$$

The second equality sign follows from the fact that any equilibrium dynamics is time reversible.

Equation (3) applies for all systems in thermal equilibrium and for all times $t_1 < t_2 < t_3$. Figure 1(a) illustrates the short-time ballistic case in which d_{13} is trivially determined by d_{12} and d_{23} because $\sqrt{d_{13}} = \sqrt{d_{12}} + \sqrt{d_{23}}$. A more interesting situation involves times of the same order of magnitude as the average relaxation time (Fig. 1(b)). In that case, while the length of $\mathbf{R}_{13}$ is always larger than that of the two other vectors, the angle between $\mathbf{R}_{12}$ and $\mathbf{R}_{23}$ is larger than $\pi/2$ because the velocity autocorrelation function for a highly viscous system is generally negative in this region of time, leading to a negative second time derivative of the MSD. A third case (Fig. 1(c)) arises when all three time differences are much larger than the average relaxation time. This results in a right-angle triangle and $d_{13} = d_{12} + d_{23}$.

We proceed to present equilibrium simulation results for a Kob-Andersen type modified binary Lennard-Jones (mBLJ) liquid [72–75]. A system of 10000 particles was simulated using the GPU software RUMD [76]. The standard Nose-Hoover thermostat was employed with a relaxation time of 0.2τ and at time step of 0.005τ (τ is the A particle LJ time unit). Data analysis was done using Julia by taking snapshots every 10 time steps.

Figure 1(d) shows a "heat map" of d_{13} as a function of d_{12} and d_{23}. As required by time reversibility, the figure is symmetrical about the $d_{12} = d_{23}$ axis. Figure 1(e) shows the relative standard deviation of d_{13} for given values of d_{12}

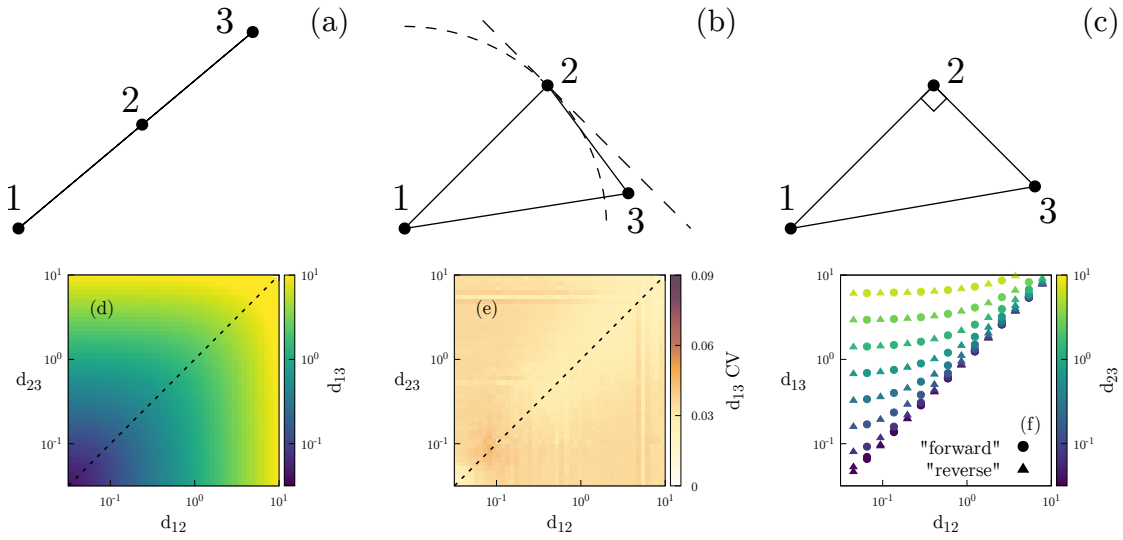

FIG. 1. Geometry of equilibrium dynamics. Panels (a), (b), (c) are schematic drawings of the positions in configuration space at three times $t_1 < t_2 < t_3$, while the numerical results reported in panels (d), (e), and (f) were obtained at $T = 0.60$ for the modified Kob-Andersen binary Lennard-Jones system (mbLJ) [72]. (a) shows the ballistic regime of free flight at very short time intervals. (b) illustrates the situation when time intervals are comparable to the average relaxation time. As explained in the text, the angle between the vectors $\mathbf{R}_{12}$ and $\mathbf{R}_{23}$ is larger than $\pi/2$ while the length of the vector $\mathbf{R}_{13}$ is larger than that of both vectors. The dashed lines mark the circle with center at $\mathbf{R}_1$ and tangent at $\mathbf{R}_2$; $\mathbf{R}_3$ must be between these as indicated in the sketch. (c) shows the situation for long time intervals in which case the vectors $\mathbf{R}_{12}$ and $\mathbf{R}_{23}$ are uncorrelated and perpendicular. This corresponds to times at which the mean-square displacement (MSD) is linear in time. (d) shows the squared lengths of the three vectors $\mathbf{R}_{12}$, $\mathbf{R}_{23}$, and $\mathbf{R}_{13}$, denoted by d_{12} etc, plotted in a "heat map" that for each value of d_{12} and d_{23} is colored according to the value of d_{13}. The diagonal symmetry is a manifestation of the time-reversal invariance of equilibrium dynamics. (e) A plot of the coefficient of variation (CV) of d_{13} for given values of d_{12} and d_{23} (the relative standard deviation). This quantity is small throughout, which shows that d_{12} and d_{23} determine d_{13}, i.e., that the "unique-triangle property" applies in equilibrium. (f) shows d_{13} as a function of d_{12} for given values of d_{23} (colors). Time reversibility implies that "forward" and "reverse" must follow the same curves, which is confirmed by the data.

and d_{23} ("CV" for coefficient of variation). The fluctuations are minute. This confirms the unique-triangle property which, as mentioned, always applies in equilibrium. Based on the same data, Fig. 1(f) shows how d_{13} depends on d_{12} (circles) for given values of d_{23} (different colors) and how d_{13} depends on d_{23} for given values of d_{12} (squares). The collapse is a consequence of time reversibility. We emphasize again that these results apply rigorously, so the simulations merely illustrate well-known facts and identities.

Other distance measures than the MSD may be used. In particular, we are interested in measures based on the inherent dynamics [77]. Recall that each configuration $\mathbf{R}(t)$ may be quenched by following the steepest descent "downhill" to the nearest potential-energy minimum. This results in the configuration's so-called inherent state [78]. In this way the inherent dynamics $\mathbf{R}^{\mathrm{I}}(t)$ is defined [77], and in terms of this quantity one may define the alternative distance d_{12}^I between the configurations at times t_1 and t_2,

$$d_{12}^I = \frac{(\mathbf{R}_2^{\mathrm{I}} - \mathbf{R}_1^{\mathrm{I}})^2}{N} \,. \tag{4}$$

Simulation results for the equilibrium inherent MSD (not shown) are analogous to those of Fig. 1 for the equilibrium MSD by obeying geometric reversibility and the unique-triangle property.

III. PHYSICAL AGING

According to the TN formalism, an aging material responds in a certain sense linearly to external stimuli like a temperature variation. Suppose the externally controlled input "effort" (field) is denoted by $e_b(t)$ (e.g., temperature, electric field, shear stress, ...) while the output "charge" is denoted by $q_a(t)$ (e.g., heat/entropy, dipole moment, shear displacement, ...). We allow for $a \neq b$ corresponding to different energy bonds [79–82]. The TN equation is then the

following Stieltjes-type convolution integral in which δ is the variation from the equilibrium value and $\xi = \xi(t)$ is the material time,

$$\delta q_a(t) \;=\; \int_{-\infty}^{\xi(t)} \psi_{ab}(\xi(t) - \xi')\, \delta e_b(\xi')\,. \tag{5}$$

This can be rewritten in the following more familiar form [4, 9]

$$\delta q_a(t) \;=\; \int_{-\infty}^{\xi(t)} \psi_{ab}(\xi(t) - \xi')\, \frac{de_b(\xi')}{d\xi'}\, d\xi'\,. \tag{6}$$

The TN description accounts well for all important aging characteristics like the asymmetry of approach and the Ritland-Kovacs crossover effect [3, 9, 62]. The most used version of the TN formalism assumes that the aging rate is a function of the property monitored [4, 5, 9, 17, 83, 84]. In the "single-parameter-aging" case this function is a simple exponential [61, 84–86].

Previous publications have focused on applying the TN formalism, not on understanding the material time. This paper investigates the possibility of defining ξ in terms of a distance measure in configuration space. In the 1990s Kurchan and Cugliandolo proposed closely related ideas in the context of spin glass models, which they studied by means of sophisticated theoretical techniques [65, 66, 70]. More recently, Schober interpreted and discussed aging simulations in terms of the MSD [67–69]. We return to these and other relevant earlier works in Sec. V A.

Suppose the material time is controlled by some distance measure d_{12} such that the difference in material time corresponding to the actual times $t_1 < t_2$ is a function of d_{12}:

$$\xi(t_2) - \xi(t_1) \;=\; f(d_{12})\,. \tag{7}$$

Here d_{12} may be defined in terms of the MSD of Eq. (1), the inherent MSD of Eq. (4), or any other distance measure obeying Eq. (2) (for simplicity we henceforth denote any such measure by the generic symbol d_{12} or simply d). How can one test in a simulation whether Eq. (7) is realistic? We proceed to show that Eq. (7) implies the so-called unique-triangle property [71], which is the first equality sign of Eq. (3), as well as the symmetry expressed by the second equality sign that is referred to as "geometric reversibility".

Consider an aging system at three times $t_1 < t_2 < t_3$ with the corresponding material times $\xi(t_1) < \xi(t_2) < \xi(t_3)$. Then Eq. (7) implies

$$\begin{aligned} \xi(t_2) - \xi(t_1) \;&=\; f(d_{12}) \\ \xi(t_3) - \xi(t_2) \;&=\; f(d_{23}) \\ \xi(t_3) - \xi(t_1) \;&=\; f(d_{13})\,. \end{aligned} \tag{8}$$

Since $\xi(t_3) - \xi(t_1) = \xi(t_3) - \xi(t_2) + \xi(t_2) - \xi(t_1)$, the two distances d_{12} and d_{23} determine the third, d_{13}. This establishes the first equality sign of Eq. (3), the unique-triangle property. A special case is that of thermal equilibrium for which the material time is proportional to the actual time. Because of this, the same function F in Eq. (3) describes equilibrium and aging.

To show the second equality sign of Eq. (3), we note that a time t_4 exists such that $\xi(t_4) - \xi(t_1) = \xi(t_3) - \xi(t_2)$. This implies $d_{14} = d_{23}$, and because $\xi(t_3) - \xi(t_4) = \xi(t_2) - \xi(t_1)$ one likewise has $d_{43} = d_{12}$. Since $\xi(t_3) - \xi(t_1) = \xi(t_3) - \xi(t_4) + \xi(t_4) - \xi(t_1)$, the distances d_{14} and d_{43} determine d_{13}, i.e., $d_{13} = F(d_{14}, d_{43}) = F(d_{23}, d_{12})$.

Which measure of the material time should be used, the standard MSD, a measure based on the inherent particle displacements, or something else? If the temperature is changed discontinuously to a higher value, the MSD changes within picoseconds because the vibrational degrees of freedom thermalize quickly. The physical idea behind the material time, however, allows only for slow and gradual changes because ξ variations are assumed to reflect *structural* changes [4, 9]. This issue is avoided by using an inherent displacement measure because the inherent state does not change on the very fast time scale. We henceforth focus on inherent displacement measures.

Turning to physical-aging data for the inherent dynamics, Fig. 2(a) shows two time-asymmetric cyclic temperature protocols switching between $T = 0.50$ and $T = 0.70$ with a period that is of the same order of magnitude as the average relaxation time at $T = 0.60$. To get good statistics, we average over many periods. Figure 2(b) shows the heat map of the inherent MSD for the fast-heating protocol. The picture is very similar to that of thermal equilibrium. In particular, the data demonstrate geometric reversibility, which is far from trivial. Similar data are obtained for the

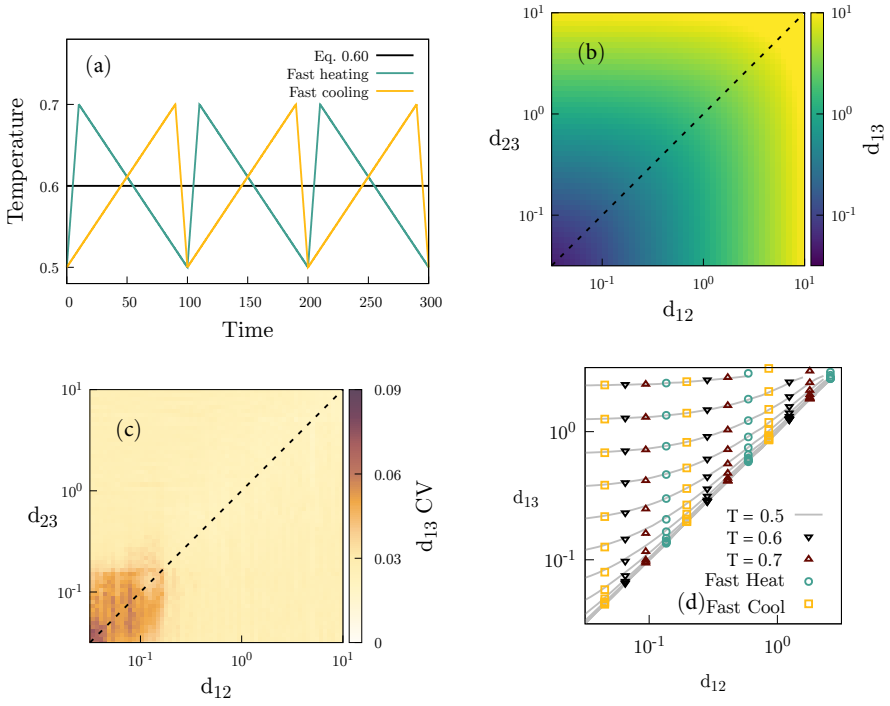

FIG. 2. Geometry of aging inherent dynamics. (a) shows two time-asymmetric temperature protocols with, respectively, fast heating and fast cooling between $T = 0.5$ and $T = 0.7$. The period was chosen to be comparable to the average relaxation time at $T = 0.60$; this means that the system is virtually in equilibrium at the higher temperatures but essentially frozen at the lower temperatures. (b) shows a heat map like that of Fig. 1 for the fast heating protocol. It is not time-reversible so the observed geometric-reversibility symmetry is not a given. (c) reports the coefficient of variation for both temperature protocols. The fact that CV is small shows that that the unique-triangle property applies to a good approximation. (d) shows a plot like that of Fig. 1(f) of d_{13} as a function of d_{12} for given values of d_{23}. Data for both aging protocols of (a) are shown together with equilibrium data at $T = 0.5$, $T = 0.6$, and $T = 0.7$. The data collapse demonstrates that the relation between the lengths of the 1,2,3 triangle are the same during aging as in equilibrium.

yellow fast-cooling protocol (not shown). Figure 2(c) shows the analog of Fig. 1(e) for both temperature protocols of (a). We see a generally good data collapse. Finally, Fig. 2(d) shows d_{13} as a function of d_{12} for different fixed values of d_{23}. The gray lines are the equilibrium curves at $T = 0.50$; the other equilibrium and aging data follow these lines. This confirms the unique-triangle property Eq. (3) for aging and shows, moreover, that the same quantitative relation between the three distances applies in equilibrium and during aging.

Having established the unique-triangle property and geometric reversibility for aging situations using the distance measure derived from the inherent MSD, we proceed to interpret aging data in view of the distance-as-time philosophy. The property monitored is the potential energy U, which is the "charge" on the left-hand side of Eq. (5), temperature is the externally controlled field. Temperature jumps imposed at $t = 0$ are studied for the mBLJ system. After a jump one monitors how $U(t)$ approaches the equilibrium value. For a jump at $t = 0$ of magnitude ΔT from an initial temperature T_i to temperature T, we define the normalized relaxation function $R(t)$ by

$$R(t) \;=\; \frac{U(t) - U_{\rm eq}(T)}{U_{\rm eq}(T_i) - U_{\rm eq}(T)}\,. \tag{9}$$

Clearly, $R(t)$ goes from unity at $t = 0$ to zero as $t \to \infty$. The prediction of the TN formalism Eq. (5) is that $R(t)$ is the same function of the material time for all temperature jumps, i.e., that for some unique function $J(\xi)$ one has

$$R(t) \;=\; J(\xi)\,. \tag{10}$$

Here ξ is the increase in material time since the jump was initiated, i.e., $\xi = \xi(t) - \xi(0)$, and $J(\xi) \equiv \psi_{ab}(\xi)/C_V$ (in the present case we have just a single energy bond, i.e., $a = b$; $C_V = \Delta U/\Delta T$ is the specific heat that is assumed to be temperature independent).

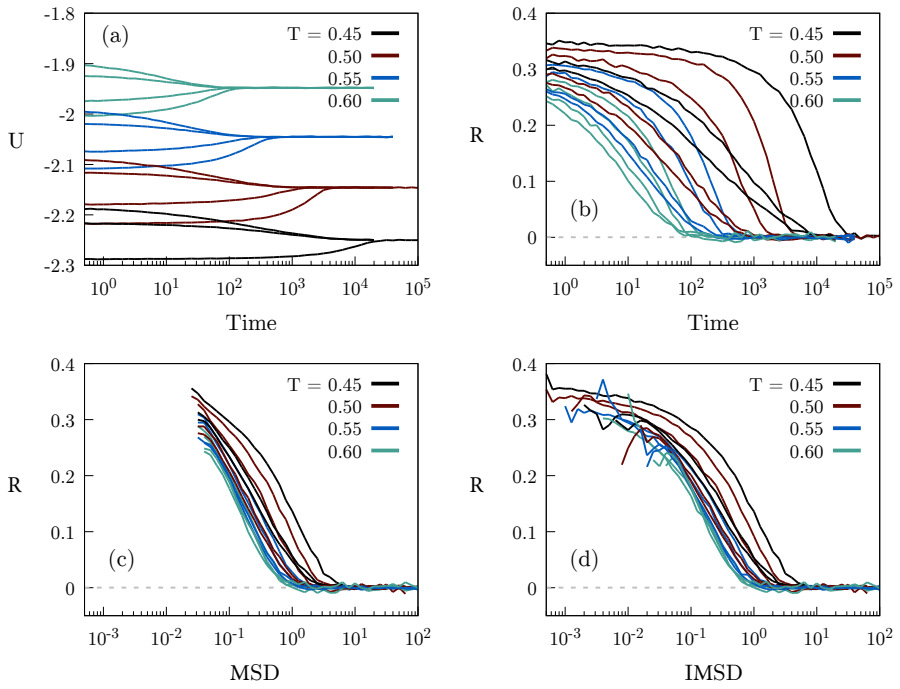

FIG. 3. Results from temperature-jump simulations. The quantity monitored is the potential energy U where the color signals the final temperature T. Jumps of magnitude ± 0.05 and ± 0.10 were studied (at $T = 0.35$ no equilibrium data are available so no jump starts here). (a) The potential energy as a function of the time after each jump was initiated. (b) The corresponding normalized relaxation functions $R(t)$ (Eq. (9)). The data cover roughly 3.5 decades of relaxation times. (c) R plotted as a function of the MSD. (d) R plotted as a function of the inherent mean-square displacement IMSD.

Figure 3(a) presents data for $U(t)$ following jumps of magnitudes ± 0.05 and ± 0.10 to $T = 0.45$, 0.50, 0.55, and 0.60, plotted as a function of the time after each jump was initiated. Jumps from higher temperatures thermalize more quickly than those coming from below; this is the asymmetry of approach seen in numerous experiments [17]. Also as in experiments, the system takes much longer time to equilibrate as T is lowered, which reflects the well-known slowing down of the dynamics of the supercooled Kob-Andersen model [73]. Figure 3(b) shows the corresponding normalized relaxation functions $R(t)$. These do not start in unity because there is a sizable, almost instantaneous change of the potential energy coming from the vibrational degrees of freedom that quickly thermalize.

Figure 3(c) uses the standard MSD for defining the material time by plotting the normalized relaxation function as a function of the MSD to investigate whether the data collapse in terms of the material time (Eq. (10)). Although the data vary just a single decade compared to the 3.5 decades in time (Fig. 3(b)), one cannot say that there is a good collapse because there is a systematic tendency for the thermalization at lower temperatures to be more "slow" than that at higher temperatures. Besides, as already mentioned, a material time defined from the standard MSD will jump virtually discontinuously if the temperature jumps; for this reason alone, the MSD is not a serious candidate for a geometric definition of the material time.

Figure 3(d) shows the same data plotted versus the inherent MSD, which does not have an unphysical jump at $t = 0$. This does not provide a better data collapse, however, but we note a different shape of the curves at short times compared to those of Fig. 3(c); the approach to the short-time plateaus of the original data is now visible. Nevertheless, neither the standard nor the inherent MSD provide a good measure of the material time.

IV. ROLE OF DYNAMIC HETEROGENEITIES

This section proposes a physical explanation for why the above two definitions of the material time do not work well in collapsing the normalized relaxation functions. It is known that relaxation in supercooled liquids and glasses does not take place in a spatially homogeneous fashion [87, 88]. At any given time there are regions with many particle rearrangements and regions with few. For the equilibrium viscous liquid, after a time that is of order the overall average structural relaxation time, fast regions become slow and *vice versa*. This fact is referred to as dynamic heterogeneity. It has been documented in several experiments and computer simulations over the last 25 years [87–89].

Dynamic heterogeneity has also been discussed in connection with theories for physical aging [24, 26, 41, 66, 83, 90]. A simple way to understand how spatial heterogeneity may influence the dynamics is via elastic models of glass-forming liquids [91–93]: because a liquid is disordered, there must be regions of varying softness [94, 95], leading to different barriers for molecular rearrangements [83, 96] and thus spatially varying levels of activity in the form of molecular motion.

The material-time concept was devised long before dynamic heterogeneity came into focus. Attempts have been made to model physical aging in terms of local material times with aging rates that vary in space [66, 97]. We here adopt a different path. The idea is that as long as a percolating structure exists of particles that have not (or almost not) moved in a given time interval, the structural memory is largely maintained. This suggests that the slowest moving particles control the material time whereas fast-moving particles or even strings of such particles [98–100] are less important for the structural relaxation. For instance, the movement of a string of particles in a fixed structure cannot be expected to change the potential energy very much or to relax significantly an overall shear stress. The assumption is that "the presence of long-lived bonded structures within the liquid may provide the long-sought connection between local structure and global dynamics" [101]. We identify these structures as the particles that have moved the shortest distance in their inherent motion. A closely related idea based on a machine-learnt "softness" parameter was discussed by Schoenholz *et al.* [83], and the importance of the slowest particles was also emphasized by Szamel and coworkers [102, 103]. In fact, the idea that the slowest particles dominate structural relaxation is more than 30 years old, see e.g., Ref. 99 and references therein. Thus Stillinger in 1988 proposed a picture according to which a glass-forming liquid "is viewed as a dynamic patchwork of relatively strongly bonded (but amorphous) molecular domains that are separated by irregular walls of weakened bonds" [104]. As a consequence, he suggested that the Stokes-Einstein relation between viscosity and diffusion coefficient (see, e.g., Ref. 105 and its references) is violated by predicting too small a diffusion coefficient because the fast particles contribute a lot to the MSD, but not very much to the overall stress relaxation. This prediction was subsequently confirmed [87, 106–109].

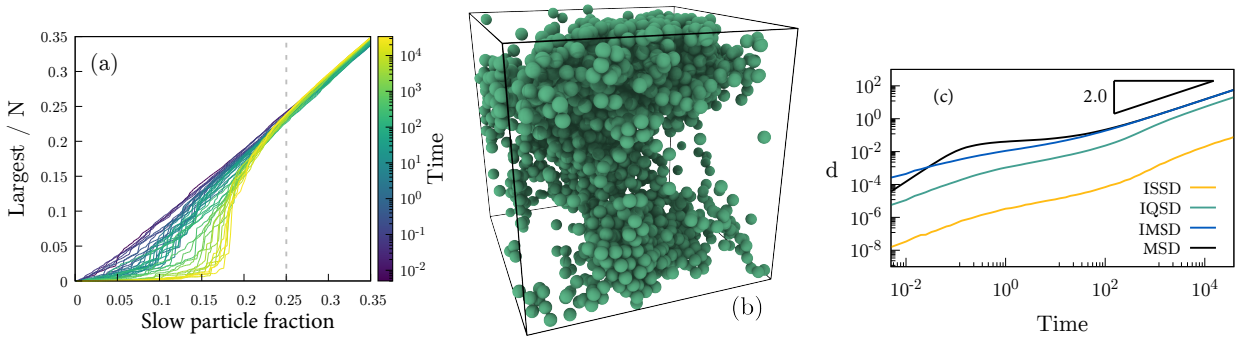

FIG. 4. Geometry of the slowest particles based on thermal-equilibrium data at $T = 0.50$. For any given time interval, the particles are sorted according to how far they have moved and subsequently assigned the same cluster if they are within the first coordination shell of each other, i.e., closer than the first minimum of the radial distribution function. (a) shows for several time intervals the relative size of the largest cluster as a function of the fraction of slowest particles. For fractions above 0.25, the largest cluster always contains a number of particles close to the total number of particles N, meaning that it percolates the sample. (b) A typical cluster of slow particles percolating the sample. (c) Different mean-square distance measures in equilibrium at $T = 0.50$ plotted as a function of time in a log-log plot. The black curve is the standard MSD for which one observes a short-time ballistic regime of slope 2, a "vibrational" plateau at intermediate times, and finally a diffusive regime at large times. The inherent MSD (IMSD) is the blue curve that has no ballistic regime but follows accurately the MSD at long times. The green curve is the inherent quartile square displacement (IQSD), i.e., the square displacement of the slowest 25% of the particles. The yellow curve is the square displacement of the single slowest particle (ISSD). At long times we see the expected slope unity for all four curves, demonstrating that distance measures based on either of them obey Eq. (2).

To combine the above physical picture with the inherent distance-as-time approach to the modeling of physical aging, we first estimate how large a fraction of slow particles is needed to form a percolating structure. We define two particles to belong to the same cluster if their distance is smaller than the first minimum of the radial distribution function. This organizes any set of particles into clusters. Focusing on the slowest particles over a given time interval, we proceed to investigate how large the largest cluster is at the end of the time interval in question. For thermal-equilibrium data at $T = 0.50$, Fig. 4(a) shows this size relative to the total number of particles ($N = 10000$) plotted as a function of the fraction of slow particles for different time intervals (colored curves). If there is a percolating structure of slow particles, the largest cluster contains a number of particles comparable to the total number of slow particles, corresponding to the line $x = y$ in the figure. Not surprisingly, for short time intervals this happens for any fraction. For longer time intervals there is only percolation of the slowest particles above a certain fraction. Based

on the figure we propose that in order to ensure percolation on all time scales, the (inherent) dynamics of the slowest 25% particles controls the material time. This threshold value is reasonable if the slow particles define compact and roughly spherical regions as previously reported [98, 99]; thus depending on the system (lattice, off-lattice, etc), percolation in three dimensions takes place at fractions typically in the range 0.2-0.3.

When a rigid structure percolates, one speaks of "rigidity percolation" as first discussed in connection with chalcogenide and other covalently bonded glasses [110–112]. Inspired by this, the name "dynamic rigidity percolation" was introduced in 1989 to explain the frequency dependence of the sound velocity in a system of inverted micelles [113]. This name signals what we suggest control the physical aging. Note that that the percolating rigid structure changes with time as reflected by the fact that the collection of slow particles changes continuously. A similar reasoning is due to Higler *et al.*, who proposed that the presence of long-lived bonded structures within the liquid provides the connection between local structure and global dynamics [101]. In a flow situation, the rheological response is controlled by long-lived structures, i.e., the rearrangement and breaking of cages of nearest neighbors [104, 114] (see also Ref. 115 for thermodynamic consequences).

Figure 4(b) shows a picture of a typical percolating structure of slow particles. Figure 4(c) compares different distance measures at equilibrium at $T = 0.50$ by showing data for the standard MSD (black), the inherent MSD (blue), the MSD of the slowest quartile (green), and the MSD of the single slowest particle (yellow). At long times all distance measures are proportional to time, i.e., obey Eq. (2), which is necessary for the defining a consistent geometric material time (see Sec. V B).

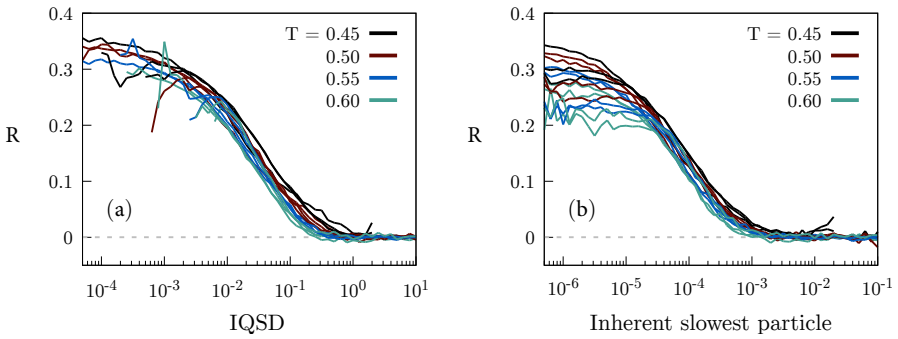

FIG. 5. Slow-particle control of the material time. (a) The normalized relaxation function of the data of Fig. 3(a) plotted as a function of the slowest inherent quartile square displacement (IQSD). We see significantly better data collapse than in Fig. 3(c) and (d), although not a perfect collapse. (b) Similar figure with the x-axis giving the inherent single slowest-particle MSD. At long times the collapse is as good as for the IQSD, but at short times the higher-temperature data level off at too low a value, showing that a material time based on the slowest particle does not work well here.

The conjecture that dynamic rigidity percolation controls aging is tested in Fig. 5(a), plotting the aging data as a function of the slowest inherent quartile square displacement of the particles. We see a significantly better collapse than for the full IMSD (Fig. 3(d)), confirming that the slowest particles are most important for the aging. Interestingly, the collapse is not strongly dependent on the exact fraction of slow particles defining the material time. Even taking the single slowest particle's (inherent) square displacement ass distance measure leads to Fig. 5(b), which is not much different from Fig. 5(a) except for not being able to capture the short-time behavior correctly. One can also instead of the IQSD use the inherent median-square displacement and get almost as good a collapse (data not shown).

V. DISCUSSION

We proceed to put the above findings into perspective by discussing their relation to related ideas and by "deriving" the TN equation from minimal assumptions.

A. Relation to previous time-as-distance proposals

As mentioned, it is not a new idea to quantify a time interval in terms of how far a system's particles have moved. This section discusses relevant previous works by first considering the linear-response case and thereafter that of physical aging.

Linear-response theory is well understood since long, founded in the fluctuation-dissipation (FD) theorem according to which the response is determined by a thermal-equilibrium time-correlation function [116]. In the simplest case, that of a single energy bond, the response is determined by an equilibrium autocorrelation function of some quantity A, denoted by $\langle A(t)A(t')\rangle$. For instance, if the externally controlled field is an electric field and the output is the current, A is the current. Another well-known is example is when the externally controlled field is the shear rate and the measured quantity is the shear stress, in which case A is the shear stress.

According to the FD theorem, the convolution kernel of the linear-response integral is the relevant time-autocorrelation function. For a glass-forming liquid, the linear responses of different quantities slow down dramatically when the temperature is lowered, often in such a way that their average relaxation times are strictly proportional in the temperature variation [117, 118]. Another characteristic feature often observed is *time-temperature superposition* (TTS). We proceed to argue that these characteristics find a natural explanation in the distance-as-time approach [119, 120].

The fact that any equilibrium time-autocorrelation function $\langle A(t')A(t)\rangle$ $(t' < t)$ goes to zero as $t - t' \to \infty$ has the geometric interpretation that the memory of a system's properties at time t' fades as the particles move away from their positions at t'. Because of this, it is an obvious idea to regard the convolution kernel of linear-response theory as a function of the distance traveled in configuration space [120]. This idea is present already in a paper by Haan from 1979 [119], which proposed to describe particle motion in a liquid by means of a Smoluchowski equation in which the role of time is played by the single-particle MSD over the time interval in question.

As we saw in Sec. II, in thermal equilibrium the distance traveled is in a one-to-one correspondence with the time that has passed, implying that the geometric viewpoint must be correct in the sense that any autocorrelation function $\langle A(0)A(t)\rangle$ is a unique function of the distance traveled in the time t. If the "geometric" equilibrium autocorrelation function is denoted by $\phi_A(R)$ where R is the distance between two points in configuration space, one has $\langle A(0)A(t)\rangle = \phi_A(R(t))$ in which $R(t)$ is the distance between two points along the equilibrium trajectory the time t apart [120]. As formulated here, this is a tautology. Nevertheless, it provides a simple rationalization of TTS because TTS applies for any quantities A if 1) the MSD obeys TTS and 2) $\phi_A(R)$ is temperature independent. The fact that different linear-response quantities slow down in a concerted fashion [117, 118] follows if the relevant geometric autocorrelation functions are temperature independent; in that case the slowing down is controlled entirely by the slowing down of the particle motion. Two interesting special cases are the following [120]. 1) If there is a Gaussian long-distance decay of the "geometric" equilibrium autocorrelation function, i.e., if $\ln(\phi_A(R)) \propto -R^2$ for $R \to \infty$, then the autocorrelation function has a long-time simple exponential decay because $R^2(t) \propto t$. Such a decay corresponds to a Debye frequency-dependence of the linear response, which is usually close to what is observed below the relevant loss peak [118, 121]. 2) If there is a simple exponential long-distance decay of the geometric equilibrium autocorrelation function, i.e., $\ln(\phi_A(R)) \propto -R$ for $R \to \infty$ [122, 123], the long-time behavior corresponds to a stretched exponential with exponent 1/2, which fits many experiments well [124–126].

Turning now to aging, as previously mentioned the main ingredients of Sec. III are present in pioneering papers by Cugliandolo, Kurchan (CK), and coworkers from the 1990s [65, 70, 127]. These authors developed a theory of physical aging of the infinite range Sherrington-Kirkpatrick spin glass based on the Schwinger–Dyson equations for both correlations and susceptibility, utilizing the fact that mean-field theory is exact for this model [66, 128]. The results obtained, which interestingly generalize to finite-range spin glasses [66], are based on a demonstration of time-scale separation and time-reparametrization invariance of the effective dynamical action describing the slow degrees of freedom; incidentally, this unusual symmetry was recently applied to models of black holes and "strange" quantum liquids [129]. The physical idea is that the proper measure of the time interval between t_1 and t_2 is not the "wall clock in the laboratory" but the value of the spin autocorrelation function $\langle S(t_1)S(t_2)\rangle$ [66]. Obviously, for Ising spins with values ± 1, the spin autocorrelation function of two configurations is in a one-to-one relation to the Euclidean distance squared between the two configurations. Thus, just as above, time intervals are quantified in terms of the distance in configuration space. Moreover, time-reparametrization invariance implies a "triangular relation" according to which for times $t_1 < t_2 < t_3$ the two spin autocorrelation functions $\langle S(t_1)S(t_2)\rangle$ and $\langle S(t_2)S(t_3)\rangle$ determine $\langle S(t_1)S(t_3)\rangle$. Because the spin autocorrelation function determines the distance, this is equivalent to the unique-triangle property Eq. (3). The analog of the above discussed geometric reversibility of aging (the second equality sign of Eq. (3)) was also arrived by CK in the form of commutativity of an algebraic relation defined from the spin autocorrelation functions [65].

Despite the similarity between the ideas of the present paper and those of CK, the present emphasis is different. CK introduced the concept of a waiting time t_w and made the seminal discovery that the relevant (e.g., spin) autocorrelation function factorizes as follows $C(t_w, t_w + \tau) = F[h(t_w)/h(t_w + \tau)]$ for some functions F and $h(t)$. This is equivalent to Eq. (7). CK focused on quenching a system from thermal equilibrium to a low temperature and not on how the system approaches equilibrium. In contrast, this is the focus of the material-time description devised for relatively small temperature perturbations. The latter description often breaks down for larger perturbations, both in experiment [9, 17, 61] and in simulations [75], which leads to an interesting question for future work: Why does a material-time description work well for relatively small perturbations of equilibrium as well as for extreme

perturbations (CK), but in many cases not in the intermediate regime? Related to this question is an additional important difference between the CK and present approaches: References 65, 66, 97, 127, and 128 emphasize that spatial heterogeneities lead to local clocks ticking with different rates: "a region looks older than another one when observed on a given time window" [66], whereas we have a single global material time and instead take the dynamic heterogeneity into account by assuming that the material time is controlled by the slowest-moving quarter of the particles.

Schober studied the aging of pressure and potential energy of the Kob-Andersen binary LJ system and found that these quantities age "in parallel", i.e., have the same normalized relaxation functions [67] (a result that illustrates the fact that this system has strong virial potential-energy correlations [130–133]). He showed that both quantities age following an exponential function of the single-particle MSD minus the vibrational MSD, which is close to the above discussed IMSD. He also found that pressure and energy follow the drop in diffusivity, in fact described by a simple exponential function. A few years later, in a study of the breakdown of the Stokes-Einstein relation between viscosity and diffusion coefficient, Schober and Peng [68] proposed to use the van Hove self-correlation function to distinguish between slow and fast particles because the latter are seen mainly in the non-Gaussian tail of the displacement distribution. The contribution of slow particles to the viscosity increases upon cooling, a result that demonstrates their importance for the highly viscous liquid phase and which is consistent with the above proposed dynamic-rigidity-percolation picture. Recently, Schober studied numerically the physical aging of liquid and amorphous selenium [69] and found that also for this system the pressure and potential energy age with a relaxation function that at long times is described by an exponential function of the MSD minus the vibrational MSD.

B. The Tool-Narayanaswamy description of aging

This section proposes an Occam's razor justification of the TN aging equation Eq. (5). In the process we relate to TTS and to the experimental fact that different linear-response functions often have the same temperature dependence. Note that TTS follows rigorously from the TN formalism, i.e., TTS is a necessary condition for TN to apply.

We start by expressing linear-response theory in terms of a distance measure d. If the externally controlled input is $e_b(t)$ and the output is $q_a(t)$, linear-response theory is expressed by

$$\delta q_a(t) \;=\; \int_{-\infty}^{t} \phi_{ab}(t-t')\,\delta e_b(t')\,. \tag{11}$$

Here, as is well known *linearity* is reflected by the fact that only the first power of the field appears, *causality* by the fact that $\delta q_a(t)$ only depends on $\delta e_b(t')$ for $t' < t$, and *time-translational invariance* by the fact that the convolution kernel ϕ_{ab} only depends on the time difference $t - t'$. By reference to Eq. (2), $t - t'$ in Eq. (11) may be replaced by a distance measure d by proceeding as follows. If one picks a fixed time in the far distant past t_0, constants α and β exist such that

$$d(t_0, t) \;=\; \alpha t + \beta\,. \tag{12}$$

This implies $t - t' = [d(t_0, t) - d(t_0, t')]\,/\alpha$. When substituted into Eq. (11) this leads to with $\psi_{ab}(x) \equiv \phi_{ab}(x/\alpha)$

$$\delta q_a(t) \;=\; \int_{-\infty}^{t} \psi_{ab}(d(t_0, t) - d(t_0, t'))\,\delta e_b(t')\,. \tag{13}$$

We emphasize that Eq. (13) is merely a reformulation of linear-response theory and is rigorously obeyed for any sufficiently small perturbation applied to any state of thermal equilibrium; also, any distance measure d obeying Eq. (2) may be used in Eq. (13).

Next we *assume* that Eq. (13) not just applies in equilibrium at a single temperature T, but also for the aging system subject to temperatures varying around T. Whether or not this is a realistic assumption depends, of course, on the choice of distance measure. The assumption has three consequences:

1. *TTS for the equilibrium linear response*
   In equilibrium at temperature T, Eq. (12) and Eq. (13) lead to

$$\delta q_a(t) \;=\; \int_{-\infty}^{t} \psi_{ab}(\alpha(T)(t-t'))\,\frac{de_b(t')}{dt'}\,dt'\,. \tag{14}$$

Writing $\delta q_a(t) = \delta q_a(\omega)\exp(i\omega t)$ and $\delta e_b(t) = \delta e_b(\omega)\exp(i\omega t)$, Eq. (14) implies $\delta q_a(\omega) = R_{ab}(\omega)\delta e_b(\omega)$ in which

$$R_{ab}(\omega) \,=\, i\omega \int_0^\infty \psi_{ab}(\alpha(T)t'')\, e^{-i\omega t''}\, dt''\,. \tag{15}$$

This implies that R_{ab} is a function of $i\omega/\alpha(T)$, i.e., TTS.

2. *Proportional time scales for different linear-response functions in thermal equilibrium*
It follows from the above that the temperature dependence of the response function $R_{ab}(\omega)$ is determined by $\alpha(T)$. This number depends only on how fast the particles move in equilibrium at temperature T, not on the quantity monitored q_a or the external field e_b. Consequently, the time scales of different linear-response functions are the same. This means that all linear-response functions that are controlled by geometry in the above sense must have the same temperature dependence of their characteristic relaxation times [117, 118].

3. *The TN formalism*
We define the material time by

$$\xi(t) \,\equiv\, d(t_0, t)\,. \tag{16}$$

Substituting this into Eq. (13) one arrives at the TN equation Eq. (5).

To summarize, if the material time via Eq. (16) is defined in terms a distance measure obeying Eq. (2), the TN formalism follows if the equation describing the equilibrium linear response also applies for out-of-equilibrium situations. This "derivation" is consistent with the fact that the TN formalism usually works best for relatively small temperature variations [9, 17, 61]. Thus our suggestion for why the TN formalism works best in the latter situation is that this regime is *pseudolinear* in the sense that the geometry of particle motion is the same as that of thermal equilibrium, compare Fig. 2(d). In other words, it is only when the "wrong" time variable is used (the laboratory time t) that physical aging violates linearity and time-translational invariance.

VI. SUMMARY

Although the TN formalism for the description of physical aging has been around for half a century and has been applied extensively in experiments and in industry, there have been few attempts to justify it theoretically. We propose that the inherent square displacement of the slowest particles is the quantity that controls the material time according to a dynamic-rigidity-percolation picture. The idea is that little overall relaxation takes place as long as a percolating structure of particles that have barely moved is maintained. None of the ingredients of our approach are new, compare Sec. V A, but they were here combined with a focus on defining Narayanaswamy's material time and explaining the origin of the TN linear convolution integral Eq. (6).

ACKNOWLEDGMENTS

This work was supported by the VILLUM Foundation's *Matter* grant (16515).

[1] F. Simon, "Über den Zustand der unterkühlten Flüssigkeiten und Gläser," Z. Anorg. Allg. Chem. **203**, 219–227 (1931).
[2] A. Q. Tool and C. G. Eichlin, "Variations caused in the heating curves of glass by heat treatment," J. Amer. Ceram. Soc. **14**, 276–308 (1931).
[3] A. J. Kovacs, "Transition vitreuse dans les polymeres amorphes. Etude phenomenologique," Fortschr. Hochpolym.-Forsch. **3**, 394–507 (1963).
[4] O. S. Narayanaswamy, "A model of structural relaxation in glass," J. Amer. Ceram. Soc. **54**, 491–498 (1971).
[5] C. T. Moynihan, P. B. Macedo, C. J. Montrose, P. K. Gupta, M. A. DeBolt, J. F. Dill, B. E. Dom, P. W. Drake, A. J. Easteal, P. B. Elterman, R. P. Moeller, H. Sasabe, and J. A. Wilder, "Structural relaxation in vitreous materials," Ann. NY Acad. Sci. **279**, 15–35 (1976).
[6] O. Mazurin, "Relaxation phenomena in glass," J. Non-Cryst. Solids **25**, 129–169 (1977).

[7] L. C. E. Struik, *Physical Aging in Amorphous Polymers and Other Materials* (Elsevier, Amsterdam, 1978).
[8] A. J. Kovacs, J. J. Aklonis, J. M. Hutchinson, and A. R. Ramos, "Isobaric volume and enthalpy recovery of glasses. II. A transparent multiparameter theory," J. Polym. Sci. Polym. Phys. **17**, 1097–1162 (1979).
[9] G. W. Scherer, *Relaxation in Glass and Composites* (Wiley, New York, 1986).
[10] I. M. Hodge, "Physical aging in polymer glasses," Science **267**, 1945–1947 (1995).
[11] C. A. Angell, K. L. Ngai, G. B. McKenna, P. F. McMillan, and S. W. Martin, "Relaxation in glassforming liquids and amorphous solids," J. Appl. Phys. **88**, 3113–3157 (2000).
[12] V. Lubchenko and P. G. Wolynes, "Theory of aging in structural glasses," J. Chem. Phys. **121**, 2852–2865 (2004).
[13] L. Grassia and D. D'Amore, "Constitutive law describing the phenomenology of subyield mechanically stimulated glasses," Phys. Rev. E **74**, 021504 (2006).
[14] J. R. White, "Polymer ageing: physics, chemistry or engineering? Time to reflect," Comptes Rendus Chimie **9**, 1396–1408 (2006).
[15] I. Kolvin and E. Bouchbinder, "Simple nonlinear equation for structural relaxation in glasses," Phys. Rev. E **86**, 010501 (2012).
[16] Y. P. Koh and S. L Simon, "Enthalpy recovery of polystyrene: Does a long-term aging plateau exist?" Macromolecules **46**, 5815–5821 (2013).
[17] G. B. McKenna and S. L. Simon, "50th anniversary perspective: Challenges in the dynamics and kinetics of glass-forming polymers," Macromolecules **50**, 6333–6361 (2017).
[18] P. Mendoza-Méndez, E. Lázaro-Lázaro, L. E. Sánchez-Díaz, P. E. Ramírez-González, G. Pérez-Ángel, and M. Medina-Noyola, "Crossover from equilibration to aging: Nonequilibrium theory versus simulations," Phys. Rev. E **96**, 022608.
[19] K. Niss, "Mapping isobaric aging onto the equilibrium phase diagram," Phys. Rev. Lett. **119**, 115703 (2017).
[20] B. Ruta, E. Pineda, and Z. Evenson, "Relaxation processes and physical aging in metallic glasses," J. Phys.: Condens. Mat. **29**, 503002 (2017).
[21] F. Arceri, F. P. Landes, L. Berthier, and G. Biroli, "Glasses and aging: A statistical mechanics perspective," arXiv:2006.09725 (2020).
[22] J. C. Mauro, *Materials Kinetics: Transport and Rate Phenomena* (Elsevier (Amsterdan, Netherlands), 2021).
[23] C. Middleton, "Glass ages in material time," Physics Today , 14–16 (May, 2022).
[24] M. Micoulaut, "Relaxation and physical aging in network glasses: a review," Rep. Prog. Phys. **79**, 066504 (2016).
[25] J. M. Hutchinson, "Physical aging of polymers," Prog. Polym. Sci. **20**, 703–760 (1995).
[26] R. D. Priestley, C. J. Ellison, L. J. Broadbelt, and J. M. Torkelson, "Structural relaxation of polymer glasses at surfaces, interfaces, and in between," Science **309**, 456–459 (2005).
[27] L. Grassia and S. L. Simon, "Modeling volume relaxation of amorphous polymers: Modification of the equation for the relaxation time in the KAHR model," Polymer **53**, 3613–3620 (2012).
[28] D. Cangialosi, V. M. Boucher, A. Alegria, and J. Colmenero, "Physical aging in polymers and polymer nanocomposites: recent results and open questions," Soft Matter **9**, 8619–8630 (2013).
[29] H. S. Chen, "The influence of structural relaxation on the density and Young's modulus of metallic glasses," J. Appl. Phys. **49**, 3289–3291 (1978).
[30] V. A. Khonik, Yu. P. Mitrofanov, S. A. Lyakhov, D. A. Khoviv, and R. A. Konchakov, "Recovery of structural relaxation in aged metallic glass as determined by high-precision in situ shear modulus measurements," J. Appl. Phys. **105**, 123521 (2009).
[31] J. C. Qiao and J. M. Pelletier, "Dynamic mechanical relaxation in bulk metallic glasses: A review," J. Mater. Sci. Technol. **30**, 523–545 (2014).
[32] S. Küchemann, C. Liu, E. M. Dufresne, J. Shin, and R. Maaß, "Shear banding leads to accelerated aging dynamics in a metallic glass," Phys. Rev. B **97**, 014204 (2018).
[33] M. Lüttich, V. M. Giordano, S. Le Floch, E. Pineda, F. Zontone, Y. Luo, K. Samwer, and B. Ruta, "Anti-aging in ultrastable metallic glasses," Phys. Rev. Lett. **120**, 135504 (2018).
[34] L. Song, W. Xu, J. Huo, F. Li, L.-M. Wang, M. D. Ediger, and J.-Q. Wang, "Activation entropy as a key factor controlling the memory effect in glasses," Phys. Rev. Lett. **125**, 135501 (2020).
[35] P. Yiu, W. Diyatmika, N Bonninghoff, Y.-C. Lu, B.-Z. Lai, and J. P. Chu, "Thin film metallic glasses: Properties, applications and future," J. Appl. Phys. **127**, 030901 (2020).
[36] L. Lundgren, P. Svedlindh, P. Nordblad, and O. Beckman, "Dynamics of the relaxation-time spectrum in a CuMn spin-glass," Phys. Rev. Lett. **51**, 911–914 (1983).
[37] L. Berthier and J.-P. Bouchaud, "Geometrical aspects of aging and rejuvenation in the Ising spin glass: A numerical study," Phys. Rev. B **66**, 054404 (2002).
[38] O. Kircher and R. Böhmer, "Aging, rejuvenation, and memory phenomena in a lead-based relaxor ferroelectric," Eur. Phys. J. B **26**, 329–338 (2002).
[39] S. M. Fielding, P. Sollich, and M. E. Cates, "Aging and rheology in soft materials," J. Rheol. **44**, 323–369 (2000).
[40] G. Foffi, E. Zaccarelli, S. Buldyrev, F. Sciortino, and P. Tartaglia, "Aging in short-ranged attractive colloids: A numerical study," J. Chem. Phys. **120**, 8824–8830 (2004).
[41] R. Pastore, C. Siviello, and D. Larobina, "Elastic and dynamic heterogeneity in aging alginate gels," Polymers **13** (2021), 10.3390/polym13213618.
[42] R. Mandal and P. Sollich, "Multiple types of aging in active glasses," Phys. Rev. Lett. **125**, 218001 (2020).
[43] G. Janzen and L. Janssen, "Aging in thermal active glasses," arXiv:2105.05705 (2021).

[44] G. Harrison, *The Dynamic Properties of Supercooled Liquids* (Academic (New York), 1976).
[45] P. G. Debenedetti and F. H. Stillinger, "Supercooled liquids and the glass transition," Nature **410**, 259 (2001).
[46] L. Berthier and G. Biroli, "Theoretical perspective on the glass transition and amorphous materials," Rev. Mod. Phys. **83**, 587–645 (2011).
[47] C. Scalliet and L. Berthier, "Rejuvenation and memory effects in a structural glass," Phys. Rev. Lett. **122**, 255502 (2019).
[48] S. Spinner and A. Napolitano, "Further studies in the annealing of a borosilicate glass," J. Res. NBS **70A**, 147–152 (1966).
[49] C. T. Moynihan, A. J. Easteal, M. A. DeBolt, and J. Tucker, "Dependence of the fictive temperature of glass on cooling rate," J. Amer. Ceram. Soc. **59**, 12–16 (1976).
[50] E. Schlosser and A. Schönhals, "Dielectric relaxation during physical aging," Polymer **32**, 2135–2140 (1991).
[51] R. L. Leheny and S. R. Nagel, "Frequency-domain study of physical aging in a simple liquid," Phys. Rev. B **57**, 5154–5162 (1998).
[52] N. B. Olsen, J. C. Dyre, and T. Christensen, "Structural relaxation monitored by instantaneous shear modulus," Phys. Rev. Lett. **81**, 1031–1033 (1998).
[53] Y. Huang and D.R. Paul, "Physical aging of thin glassy polymer films monitored by gas permeability," Polymer **45**, 8377 – 8393 (2004).
[54] R. Di Leonardo, T. Scopigno, G. Ruocco, and U. Buontempo, "Spectroscopic cell for fast pressure jumps across the glass transition line," Rev. Sci. Instrum. **75**, 2631–2637 (2004).
[55] P. Lunkenheimer, R. Wehn, U. Schneider, and A. Loidl, "Glassy aging dynamics," Phys. Rev. Lett. **95**, 055702 (2005).
[56] C. Brun, F. Ladieu, D. L'Hote, G. Biroli, and J-P. Bouchaud, "Evidence of growing spatial correlations during the aging of glassy glycerol," Phys. Rev. Lett. **109**, 175702 (2012).
[57] B. Ruta, Y. Chushkin, G. Monaco, L. Cipelletti, E. Pineda, P. Bruna, V. M. Giordano, and M. Gonzalez-Silveira, "Atomic-scale relaxation dynamics and aging in a metallic glass probed by x-ray photon correlation spectroscopy," Phys. Rev. Lett. **109**, 165701 (2012).
[58] R. Richert, "Supercooled liquids and glasses by dielectric relaxation spectroscopy," Adv. Chem. Phys. **156**, 101–195 (2015).
[59] A. Q. Tool, "Relation between inelastic deformability and thermal expansion of glass in its annealing range," J. Amer. Ceram. Soc. **29**, 240–253 (1946).
[60] J. C. Mauro, R. J. Loucks, and P. K. Gupta, "Fictive temperature and the glassy state," J. Amer. Ceram. Soc. **92**, 75–86 (2009).
[61] B. Riechers, L. A. Roed, S. Mehri, T. S. Ingebrigtsen, T. Hecksher, J. C. Dyre, and K. Niss, "Predicting nonlinear physical aging of glasses from equilibrium relaxation via the material time," Sci. Adv. **8**, eabl9809 (2022).
[62] H. N. Ritland, "Limitations of the fictive temperature concept," J. Amer. Ceram. Soc. **39**, 403–406 (1956).
[63] I. M. Hodge, "Adam-Gibbs formulation of enthalpy relaxation near the glass transition," J. Res. Natl. Inst. Stand. Technol. **102**, 195–205 (1997).
[64] T. Hecksher, N. B. Olsen, and J. C. Dyre, "Fast contribution to the activation energy of a glass-forming liquid," Proc. Natl. Acad. Sci. (USA) **116**, 16736–16741 (2019).
[65] L. F. Cugliandolo and J. Kurchan, "On the out-of-equilibrium relaxation of the Sherrington-Kirkpatrick model," J. Phys. A: Math. Gen. **27**, 5749–5772 (1994).
[66] C. Chamon and L. F. Cugliandolo, "Fluctuations in glassy systems," J. Stat. Mech.: Theory and Experiments **7**, P07022 (2007).
[67] H. R. Schober, "Modeling aging rates in a simple glass and its melt," Phys. Rev. B **85**, 024204 (2012).
[68] H. R. Schober and H. l. Peng, "Heterogeneous diffusion, viscosity, and the Stokes-Einstein relation in binary liquids," Phys. Rev. E **93**, 052607 (2016).
[69] H. R. Schober, "Diffusion, relaxation, and aging of liquid and amorphous selenium," Phys. Rev. B **103**, 094202 (2021).
[70] C. Chamon, M. P. Kennett, H. E. Castillo, and L. F. Cugliandolo, "Separation of time scales and reparametrization invariance for aging systems," Phys. Rev. Lett. **89**, 217201 (2002).
[71] J. C. Dyre, "Narayanaswamy's 1971 aging theory and material time," J. Chem. Phys. **143**, 114507 (2015).
[72] T. B. Schrøder and J. C. Dyre, "Solid-like mean-square displacement in glass-forming liquids," J. Chem. Phys. **152**, 141101 (2020).
[73] W. Kob and H. C. Andersen, "Testing mode-coupling theory for a supercooled binary Lennard-Jones mixture I: The van Hove correlation function," Phys. Rev. E **51**, 4626–4641 (1995).
[74] W. Kob and J.-L. Barrat, "Aging effects in a Lennard-Jones glass," Phys. Rev. Lett. **78**, 4581–4584 (1997).
[75] W. Kob and J.-L. Barrat, "Fluctuations, response and aging dynamics in a simple glass-forming liquid out of equilibrium," Eur. Phys. J. B **13**, 319–333 (2000).
[76] N. P. Bailey, T. S. Ingebrigtsen, J. S. Hansen, A. A. Veldhorst, L. Bøhling, C. A. Lemarchand, A. E. Olsen, A. K. Bacher, L. Costigliola, U. R. Pedersen, H. Larsen, J. C. Dyre, and T. B. Schrøder, "RUMD: A general purpose molecular dynamics package optimized to utilize GPU hardware down to a few thousand particles," Scipost Phys. **3**, 038 (2017).
[77] T. B. Schrøder, S. Sastry, J. C. Dyre, and S. C. Glotzer, "Crossover to potential energy landscape dominated dynamics in a model glass-forming liquid," J. Chem. Phys. **112**, 9834–9840 (2000).
[78] F. H. Stillinger and T. A. Weber, "Dynamics of structural transitions in liquids," Phys. Rev. A **28**, 2408–2416 (1983).
[79] H. Paynter, *Analysis and Design of Engineering Systems* (MIT Press, Cambridge, Massachusetts, 1961).
[80] G. Oster, A. Perelson, and A. Katchalsky, "Network thermodynamics," Nature **234**, 393–399 (1971).

[81] D. C. Karnopp, D. L. Margolis, and R. C. Rosenberg, *System Dynamics – Modeling and Simulation of Mechatronic Systems*, 4th ed. (Wiley, New York, 2006).

[82] T. B. Schrøder, N. P. Bailey, U. R. Pedersen, N. Gnan, and J. C. Dyre, "Pressure-energy correlations in liquids. III. Statistical mechanics and thermodynamics of liquids with hidden scale invariance," J. Chem. Phys. **131**, 234503 (2009).

[83] S. S. Schoenholz, E. D. Cubuk, E. Kaxiras, and A. J Liu, "Relationship between local structure and relaxation in out-of-equilibrium glassy systems," Proc. Natl. Acad. Sci. (USA) **114**, 263–267 (2017).

[84] L. A. Roed, T. Hecksher, J. C. Dyre, and K. Niss, "Generalized single-parameter aging tests and their application to glycerol," J. Chem. Phys. **150**, 044501 (2019).

[85] T. Hecksher, N. B. Olsen, and J. C. Dyre, "Communication: Direct tests of single-parameter aging," J. Chem. Phys. **142**, 241103 (2015).

[86] T. Hecksher, D. H. Torchinsky, C. Klieber, J. A. Johnson, J. C. Dyre, and K. A. Nelson, "Toward broadband mechanical spectroscopy," Proceedings of the National Academy of Sciences (USA) **114**, 8710–8715 (2017).

[87] M. D. Ediger, "Spatiall heterogeneous dynamics in supercooled liquids," Ann. Rev. Phys. Chem. **51**, 99–128 (2000).

[88] L. Berthier, G. Biroli, J.-P. Bouchaud, L. Cipelletti, and W. van Saarloos, eds., *Dynamical Heterogeneities in Glasses, Colloids, and Granular Media* (Oxford Univ. Press, 2011).

[89] S. Karmakar, C. Dasgupta, and S. Sastry, "Growing length scales and their relation to timescales in glass-forming liquids," Annu. Rev. Cond. Mat. Phys. **5**, 255–284 (2014).

[90] M. Lulli, C.-S. Lee, H.-Y. Deng, C.-T. Yip, and C.-H. Lam, "Spatial heterogeneities in structural temperature cause Kovacs' expansion gap paradox in aging of glasses," Phys. Rev. Lett. **124**, 095501 (2020).

[91] J. C. Dyre, "The glass transition and elastic models of glass-forming liquids," Rev. Mod. Phys. **78**, 953–972 (2006).

[92] Asaph Widmer-Cooper and Peter Harrowell, "Predicting the long-time dynamic heterogeneity in a supercooled liquid on the basis of short-time heterogeneities," Phys. Rev. Lett. **96**, 185701 (2006).

[93] L. Larini, A. Ottochian, C. De Michele, and D. Leporini, "Universal scaling between structural relaxation and vibrational dynamics in glass-forming liquids and polymers," Nature Phys. **4**, 42–45 (2008).

[94] S. S. Schoenholz, E. D. Cubuk, D. M. Sussman, E. Kaxiras, and A. J. Liu, "A structural approach to relaxation in glassy liquids," Nat. Phys. **12**, 469–471 (2016).

[95] M. K. Nandi and S. M. Bhattacharyya, "Microscopic theory of softness in supercooled liquids," Phys. Rev. Lett. **126**, 208001 (2021).

[96] G. Kapteijns, D. Richard, E. Bouchbinder, T. B. Schrøder, J. C. Dyre, and E. Lerner, "Does mesoscopic elasticity control viscous slowing down in glassforming liquids?" J. Chem. Phys. **155**, 074502 (2021).

[97] H. E. Castillo and A. Parsaeian, "Local fluctuations in the ageing of a simple structural glass," Nat. Phys. **3**, 26–28 (2007).

[98] C. Donati, J. F. Douglas, W. Kob, S. J. Plimpton, P. H. Poole, and S. C. Glotzer, "Stringlike cooperative motion in a supercooled liquid," Phys. Rev. Lett. **80**, 2338–2341 (1998).

[99] S. C. Glotzer, "Spatially heterogeneous dynamics in liquids: insights from simulation," J. Non-Cryst. Solids **274**, 342–355 (2000).

[100] A. Shavit, J. F. Douglas, and R. A. Riggleman, "Evolution of collective motion in a model glass-forming liquid during physical aging," J. Chem. Phys. **138**, 12A528 (2013).

[101] R. Higler, J. Krausser, J. van der Gucht, A. Zaccone, and J. Sprakel, "Linking slow dynamics and microscopic connectivity in dense suspensions of charged colloids," Soft Matter **14**, 780–788 (2018).

[102] S. K. Kumar, G. Szamel, and J. F. Douglas, "Nature of the breakdown in the Stokes-Einstein relationship in a hard sphere fluid," J. Chem. Phys. **124**, 214501 (2006).

[103] G. Szamel and E. Flenner, "Time scale for the onset of Fickian diffusion in supercooled liquids," Phys. Rev. E **73**, 011504 (2006).

[104] F. H. Stillinger, "Relaxation and flow mechanisms in "fragile" glass-forming liquids," J. Chem. Phys. **89**, 6461–6469 (1988).

[105] L. Costigliola, D. M. Heyes, T. B Schrøder, and J. C. Dyre, "Revisiting the Stokes-Einstein relation without a hydrodynamic diameter," J. Chem. Phys. **150**, 021101 (2019).

[106] F. Fujara, B. Geil, H. Sillescu, and G. Fleischer, "Translational and rotational diffusion in supercooled orthoterphenyl close to the glass transition," Z. Phys. B – Cond. Mat. **88**, 195–204 (1992).

[107] M. T. Cicerone and M. D. Ediger, "Enhanced translation of probe molecules in supercooled o-terphenyl: Signature of spatially heterogeneous dynamics?" J. Chem. Phys. **104**, 7210–7218 (1996).

[108] L. Andreozzi, A. Di Schino, M. Giordano, and D. Leporini, "Evidence of a fractional Debye-Stokes-Einstein law in supercooled o-terphenyl," Europhys. Lett. **38**, 669–674 (1997).

[109] R. Yamamoto and A. Onuki, "Heterogeneous diffusion in highly supercooled liquids," Phys. Rev. Lett. **81**, 4915–4918 (1998).

[110] J. C. Phillips and M. F. Thorpe, "Constraint theory, vector percolation and glass formation," Solid State Commun. **53**, 699–702 (1985).

[111] W. Bresser, P. Boolchand, and P. Suranyi, "Rigidity percolation and molecular clustering in network glasses," Phys. Rev. Lett. **56**, 2493–2496 (1986).

[112] M. Tatsumisago, B. L. Halfpap, J. L. Green, S. M. Lindsay, and C. A. Angell, "Fragility of Ge-As-Se glass-forming liquids in relation to rigidity percolation, and the Kauzmann paradox," Phys. Rev. Lett. **64**, 1549–1552 (1990).

[113] L. Ye, D. A. Weitz, P. Sheng, S. Bhattacharya, J. S. Huang, and M. J. Higgins, "Dynamic rigidity percolation in inverted micelles," Phys. Rev. Lett. **63**, 263–266 (1989).

[114] M. Laurati, P. Maßhoff, K. J. Mutch, S. U. Egelhaaf, and A. Zaccone, "Long-lived neighbors determine the rheological response of glasses," Phys. Rev. Lett. **118**, 018002 (2017).

[115] K. Trachenko and V. V. Brazhkin, "Duality of liquids," Scientific Reports **3**, 2188 (2013).

[116] L. E. Reichl, *A Modern Course in Statistical Physics*, 4th ed. (Wiley-VCH, 2016).

[117] B. Jakobsen, T. Hecksher, T. Christensen, N. B. Olsen, J. C. Dyre, and K. Niss, "Identical temperature dependence of the time scales of several linear-response functions of two glass-forming liquids," J. Chem. Phys. **136**, 081102 (2012).

[118] L. A. Roed, J. C. Dyre, K. Niss, T. Hecksher, and B Riechers, "Time-scale ordering in hydrogen- and van der Waals-bonded liquids," J. Chem. Phys. **154**, 184508 (2021).

[119] S. W. Haan, "Dynamic behavior of pairs of atoms in simple liquids," Phys. Rev. A **20**, 2516–2520 (1979).

[120] J. C. Dyre, "A statistical mechanical approximation for the calculation of time auto-correlation functions," cond-mat/9712222 (unpublished) (1997).

[121] T. Hecksher and K. Niss, "Perspective: Searching for simplicity rather than universality in glass-forming liquids," J. Chem. Phys. **149**, 230901 (2018).

[122] E. R. Weeks, J. C. Crocker, and D. A. Weitz, "Short- and long-range correlated motion observed in colloidal glasses and liquids," J. Phys. Cond. Mat. **19**, 205131 (2007).

[123] N. P. Bailey, T. B. Schrøder, and J. C. Dyre, "Exponential distributions of collective flow-event properties in viscous liquid dynamics," Phys. Rev. Lett. **102** (2009), 10.1103/physrevlett.102.055701.

[124] J. C. Dyre, "Solidity of viscous liquids. IV. Density fluctuations," Phys. Rev. E **74**, 021502 (2006).

[125] J. C. Dyre, "Solidity of viscous liquids. V. Long-wavelength dominance of the dynamics," Phys. Rev. E **76**, 041508 (2007).

[126] A. I. Nielsen, T. Christensen, B. Jakobsen, K. Niss, N. B. Olsen, R. Richert, and J. C. Dyre, "Prevalence of approximate $\sqrt{t}$ relaxation for the dielectric α process in viscous organic liquids," J. Chem. Phys. **130**, 154508 (2009).

[127] L. F. Cugliandolo, J. Kurchan, and L. Peliti, "Energy flow, partial equilibration, and effective temperatures in systems with slow dynamics," Phys. Rev. E **55**, 3898–3914 (1997).

[128] L. F. Cugliandolo, "The effective temperature," J. Phys. A: Mathematical and Theoretical **44**, 483001 (2011).

[129] D. Facoetti, G. Biroli, J. Kurchan, and D. R. Reichman, "Classical glasses, black holes, and strange quantum liquids," Phys. Rev. B **100**, 205108 (2019).

[130] U. R. Pedersen, N. P. Bailey, T. B. Schrøder, and J. C. Dyre, "Strong pressure-energy correlations in van der Waals liquids," Phys. Rev. Lett. **100**, 015701 (2008).

[131] N. P. Bailey, U. R. Pedersen, N. Gnan, T. B. Schrøder, and J. C. Dyre, "Pressure-energy correlations in liquids. I. Results from computer simulations," J. Chem. Phys. **129**, 184507 (2008).

[132] N. Gnan, T. B. Schrøder, U. R. Pedersen, N. P. Bailey, and J. C. Dyre, "Pressure-energy correlations in liquids. IV. "Isomorphs" in liquid phase diagrams," J. Chem. Phys. **131**, 234504 (2009).

[133] U. R. Pedersen, T. B. Schrøder, and J. C. Dyre, "Phase diagram of Kob-Andersen-type binary Lennard-Jones mixtures," Phys. Rev. Lett. **120**, 165501 (2018).